Supporting Information

Boosting the acidic electrocatalytic nitrogen reduction performance of MoS$_2$ by strain engineering

Jiawei Liang,[a†] Shuangxiu Ma,[a†] Jing Li,[a] Yangang Wang,[c]* Junli Wu,[a] Quan Zhang,[a] Zhao Liu,[a] Zehui Yang,[a]* Konggang Qu[b] and Weiwei Cai[a]*

J. Liang and S. Ma contribute equally to this work.

[a]Sustainable Energy Laboratory, Faculty of Materials Science and Chemistry, China University of Geosciences, Wuhan, 430074, China. willcai1985@gmail.com (W. Cai), yeungzehui@gmail.com (Z. Yang).

[b]Shandong Provincial Key Laboratory/Collaborative Innovation Center of Chemical Energy Storage & Novel Cell Technology, Liaocheng University, Liaocheng, 252059, China.

[c]College of Biological Chemical Science and Engineering, Jiaxing University, Jiaxing, Zhejiang, 314001, China. ygwang8136@mail.zjxu.edu.cn (Y. Wang)

Physical characterizations. The micromorphology and elemental distribution of the catalyst samples were observed and contrasted by a field emission scanning electron microscopy (FESEM, Hitch SU8000, Japan) and high-resolution transmission electron microscopy (HRTEM, FEI Tecnai G2 F30; Thermo Fisher Titan Themis G2) equipped with an energy-dispersive X-ray Spectroscope (EDS, Oxford INCA x-sight, England). X-ray photoelectron spectra (XPS) were recorded using an Escalab 250XI spectrometer (ThermoFisher, USA). The specific surface area was measured by the Brunauer-Emmett-Teller (BET) method based on the N_2 adsorption isotherm measurement using a Microactive for ASAP 2460 (Micromeritics Instrument Corporation). The absorbance data of spectrophotometer were collected utilizing UV-Vis spectrophotometer. N_2-TPD detection was conducted by AutoChem 2950 HP chemical adsorption instrument.

Electrochemical measurements. Prior N_2 electrochemical reduction, Nafion 211 membrane was firstly treated to remove the impurities. Nafion 211 membrane was oxidized in 3% H_2O_2 solution at 90 °C for 1 h and boiled in ultrapure water for another 1 h, and then soaked in 0.5 M H_2SO_4 overnight. After rinsing several times with ultrapure water, the membrane was employed to isolate cathode and anode in H-type electrolytic cell device. All electrochemical measurements were performed by the Gamry interface 1000e potentiostat with a typical three-electrode system. In brief, 5 mg of the as-prepared electrocatalysts were ultrasonically dispersed in 800 μL of deionized water, 175 μL of isopropanol and 25 μL of Nafion solution for 1 h to acquire homogeneous dispersion. Thereafter, 7 μL of the resultant ink was loaded onto the surface of glassy carbon electrode with a diameter of 3 mm and then air-dried to be served as a working electrode (mass loading of 0.5 mg cm^{-2}). A graphite rod was employed as the counter electrode and saturated calomel electrode (SCE) as the reference electrode. The N_2 electrochemical reduction was performed at applied potentials for 2 h in N_2-saturated 0.05 M H_2SO_4 under room temperature. Linear sweep voltammetry (LSV) was conducted at scan rate of 5 mV s^{-1} to estimate the electrocatalytic activity for N_2 reduction in N_2 or Ar saturated

electrolyte. Cyclic voltammetry (CV) was performed between 0.16 and 0.26 V at different

scanning rates ranging from 10 to 100 mV s^{-1} to calculate the double layer capacitances (C_{dl}).

Prior to the measurement, the electrolyte was purged with N_2 or Ar for at least 30 min. All of

the potentials referred in this work were converted to values with reference to a reversible

hydrogen electrode (RHE) and the current density was normalized to the geometrical surface

area of electrode.

Quantification of ammonia. The different amount of NH_3 present was detected by the

indophenol blue method. Typically, 2 mL of electrolyte was removed for the electrolytic cell

after chronoamperometric tests. Subsequently, 2 mL of 1 M sodium hydroxide solution

containing salicylic acid (5 wt%) and sodium citrate (5 wt%) was added, followed by addition

of 1 mL of 0.05 M sodium hypochlorite and 0.2 mL of sodium nitroferricyanide solution (1

wt%). After setting aside for 1 h to fully develop color, the ultraviolet-visible (UV-vis)

absorption spectra were employed to examine the colored solution with the absorption peak at

655 nm. The concentration-absorbance curves were calibrated utilizing standard NH_3 solution

with a series of concentrations in 0.05 M H_2SO_4.

The yield rate of NH_3 production can be calculated according to the following equation:

$$v_{NH_3} = \frac{c \times V}{t \times m_{cat}}$$

The Faradaic efficiency (FE) for N_2 reduction was estimated from dividing the total charge

consumed for the electrodes by the quantity of electric charge for NH_3 production and the

total charge passed through the electrodes during the electrolysis, and the FE was calculated

using the following equation:

$$FE = \frac{3 \times F \times c \times V}{17 \times Q}$$

3

where F is the Faraday constant (96485 C mol^{-1}); c is the measured NH_3 concentration; V is the volume of the electrolyte for NH_3 collection; t is the duration of chronoamperometric test; m_{cat} is the catalyst loading mass at the work electrode; Q is the quantity of applied electricity.

Nuclear magnetic resonance (NMR) spectroscopy. In the electrocatalytic NRR experiment, Argon gas was purged to the cathodic cell to remove impurity gas and then purging for 30 min with the gas to be tested. After electrolysis at -0.2 V vs. RHE for 2 h, 50 mL of the electrolyte was taken out and acidized to pH=3 by adding H_2SO_4 (pH=1), and then concentrated to 5 mL by heating via reduced pressure distillation. Afterwards, 0.55 mL of the resulting solution was taken out and mixed with 0.05 mL D_2O for ^{1}H-NMR measurement. A total of 1024 transient scans were recorded with an interscan delay of 1 s. 64 K complex points was acquired for each FID with an acquisition time of 3.4 s. The produced ammonia was quantitatively detected by using ^{1}H-NMR means on a Bruker AVANCE III HD 400 instrument. A known amount of D_2O was used as an internal standard.

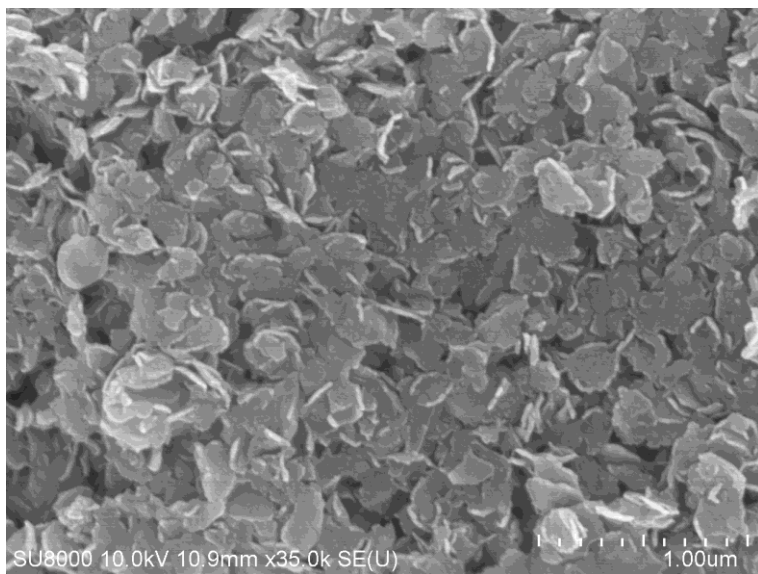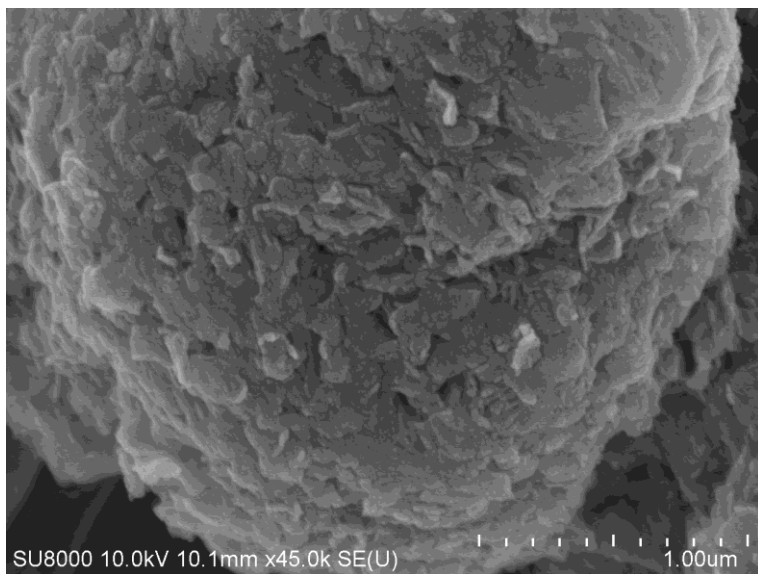Figure S1. SEM image of the pristine MoS_2.

Figure S2. SEM image of the F-MoS$_2$-2.

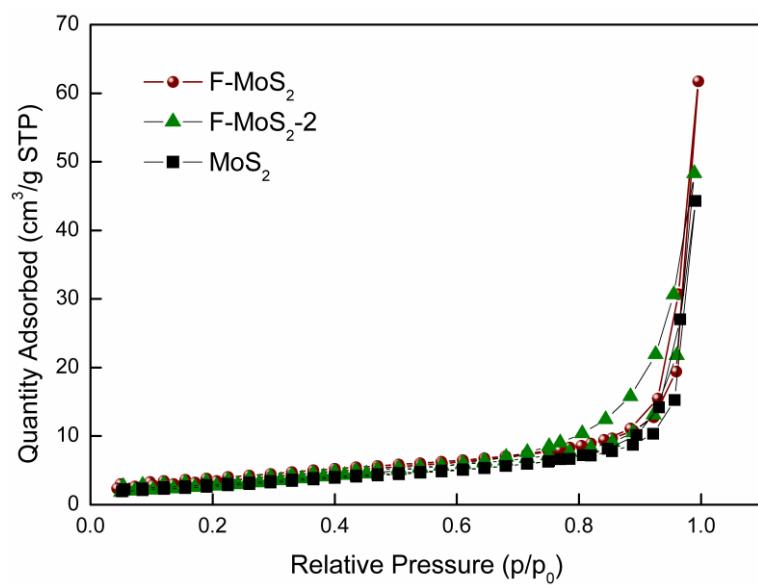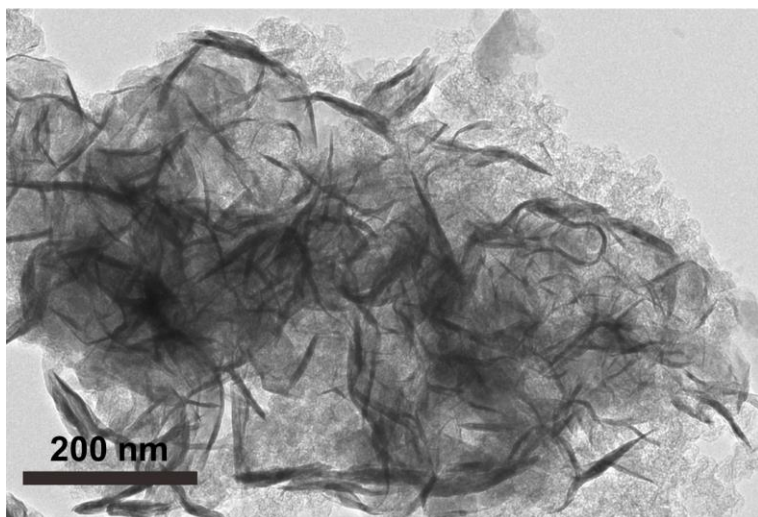Figure S3. N_2 adsorption-desorption isotherms of MoS_2, $F-MoS_2$ and $F-MoS_2$-2.
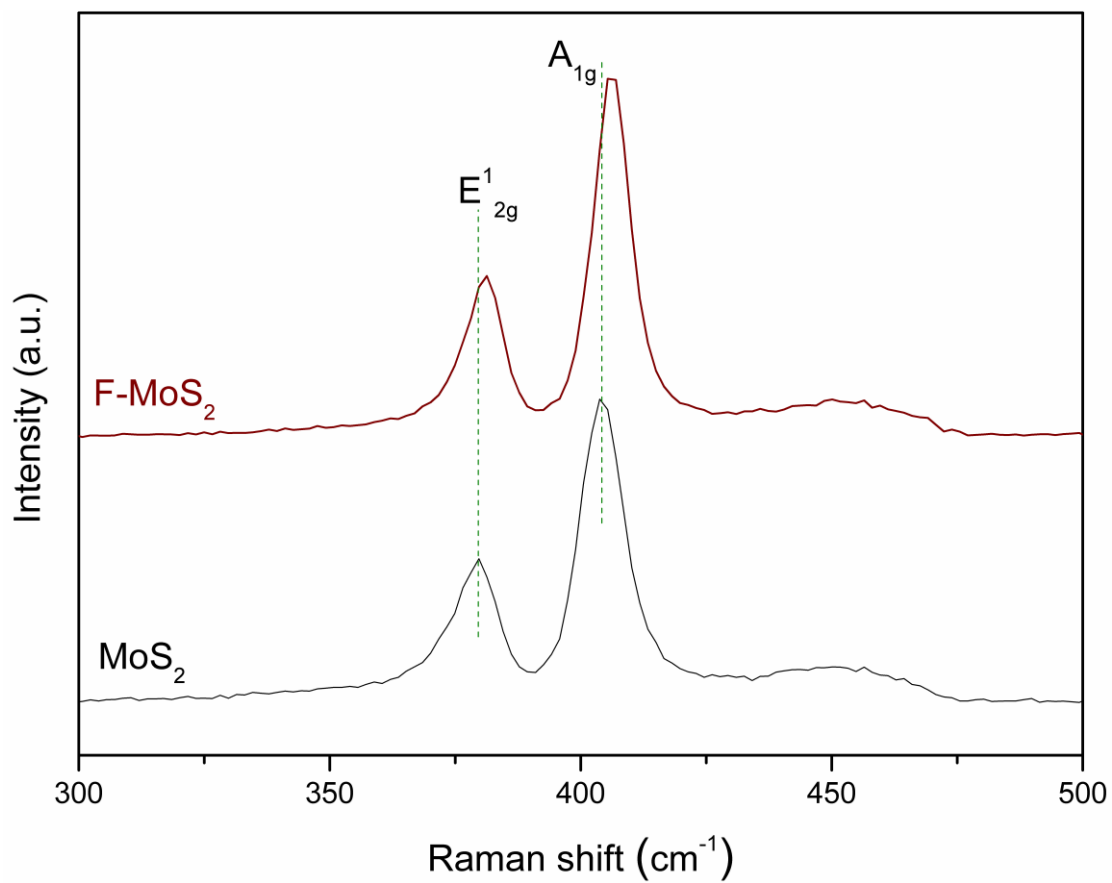
Figure S4. TEM image of the F-MoS$_2$.

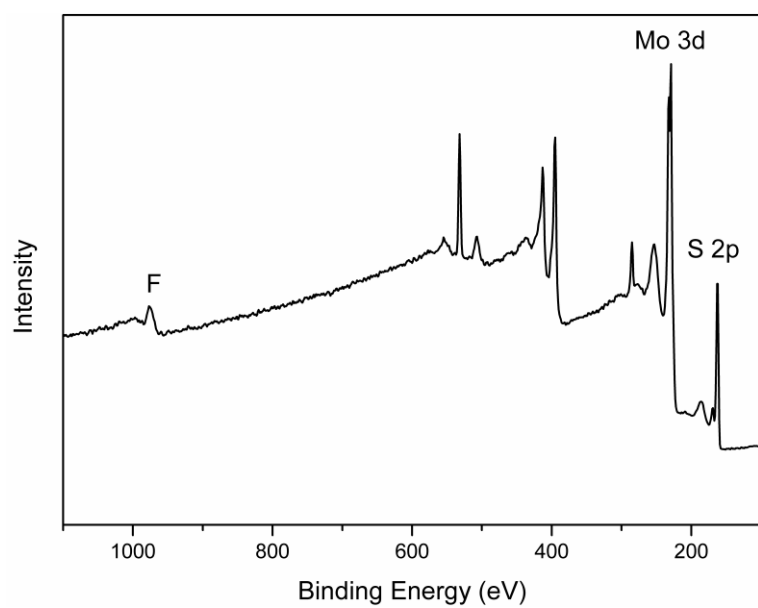Figure S5. Raman spectra of the F-MoS$_2$ and the prisitin MoS$_2$.

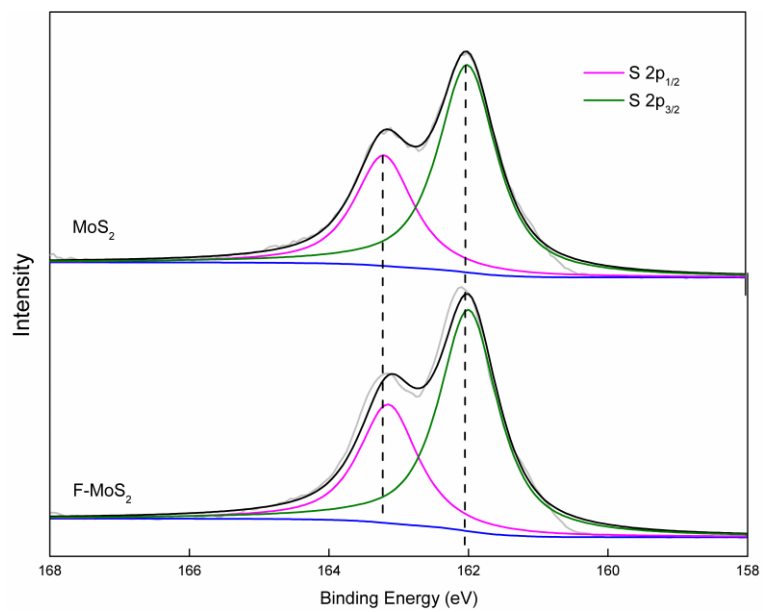Figure S6. Survey XPS spectra of the F-MoS$_2$ catalyst.

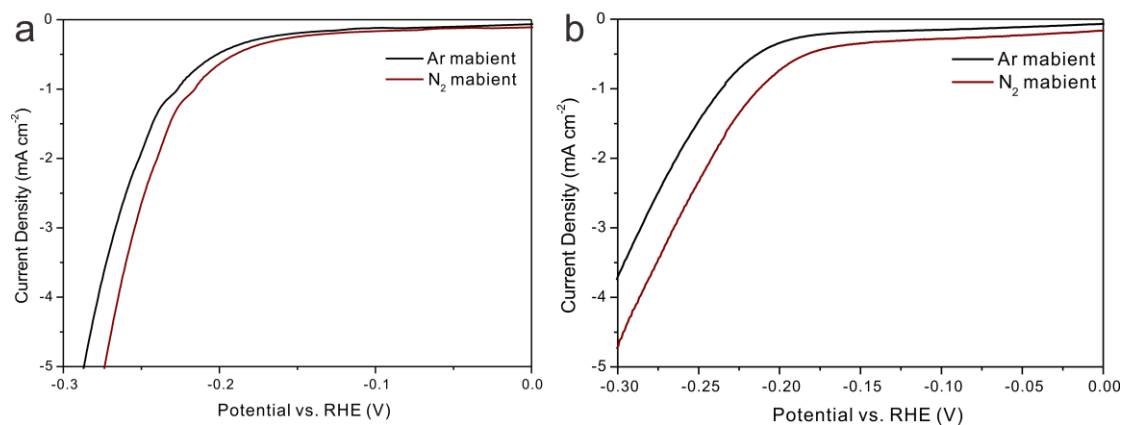Figure S7. Comparison between the S 2p XPS spectra of the pristine MoS_2 and F-MoS_2 catalysts.

Figure S8. LSV curves of (a) MoS_2 and (b) $F-MoS_2$ measured at 0.05 M H_2SO_4 saturated with Ar and N_2.
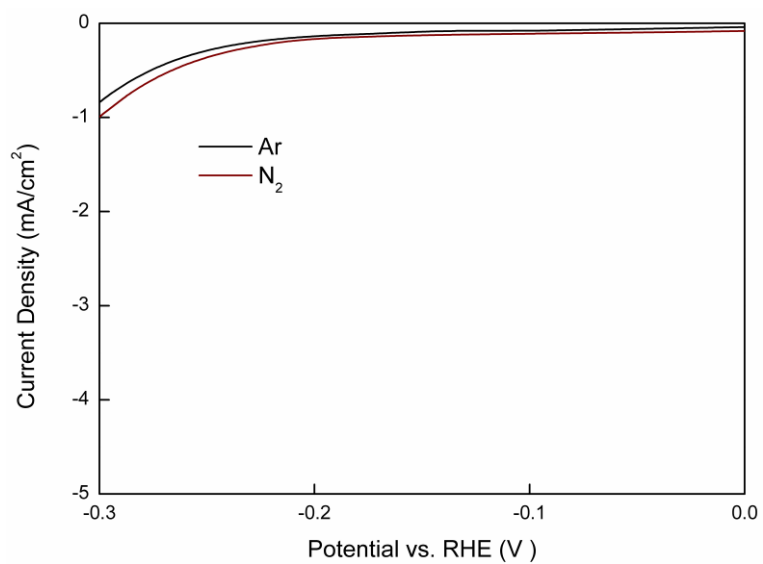
Figure S9. LSV curves of F-MoS$_2$-2 measured at 0.05 M H$_2$SO$_4$ saturated with Ar and N$_2$.
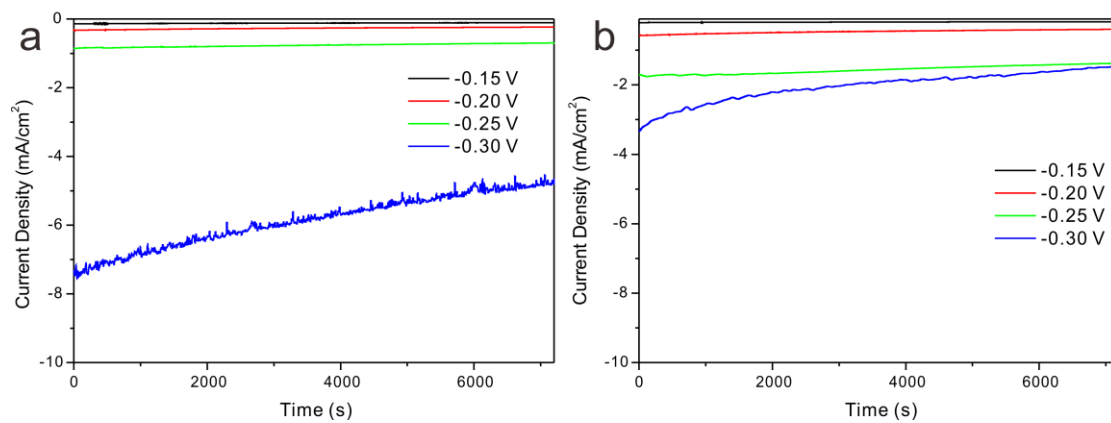
Figure S10. Chronoamperometry (CA) of (a) MoS_2 and (b) F-MoS_2 measured at -0.15V to -0.30 V vs. RHE in N_2 saturated 0.05 M H_2SO_4 solutions.
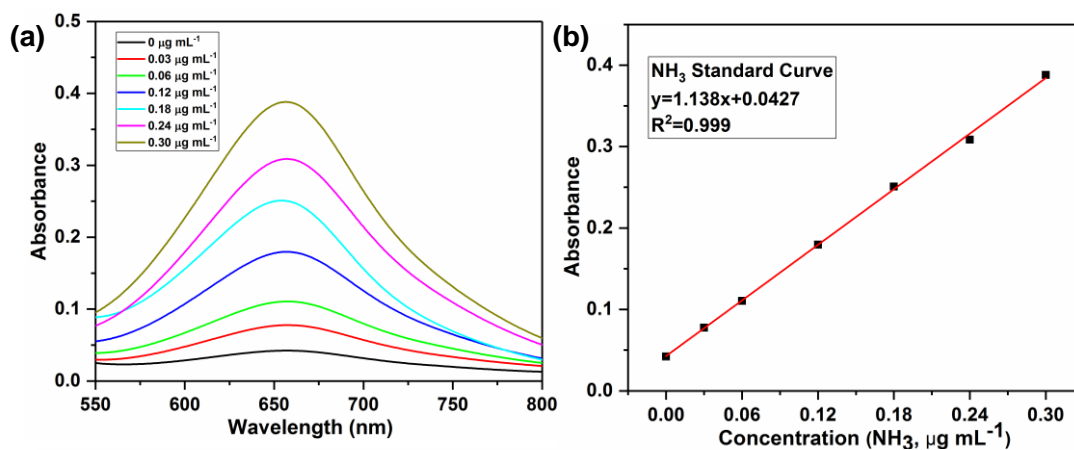
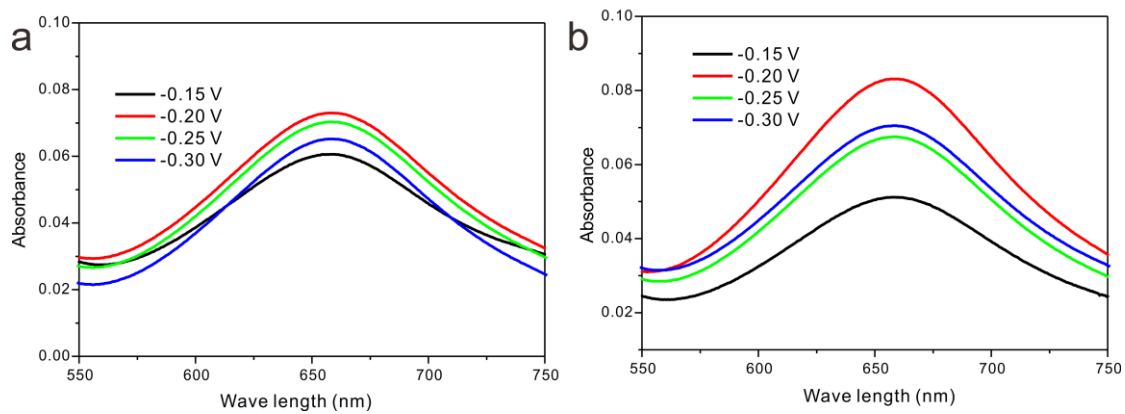Figure S11. Calibration curve for colorimetric NH₃ assay using Nessler reagent.

Figure S12. UV-vis absorption spectra of the electrolyte stained with indophenol indicator after 2 h electrolysis at a series of potentials for (a) MoS_2 and (b) $F-MoS_2$.

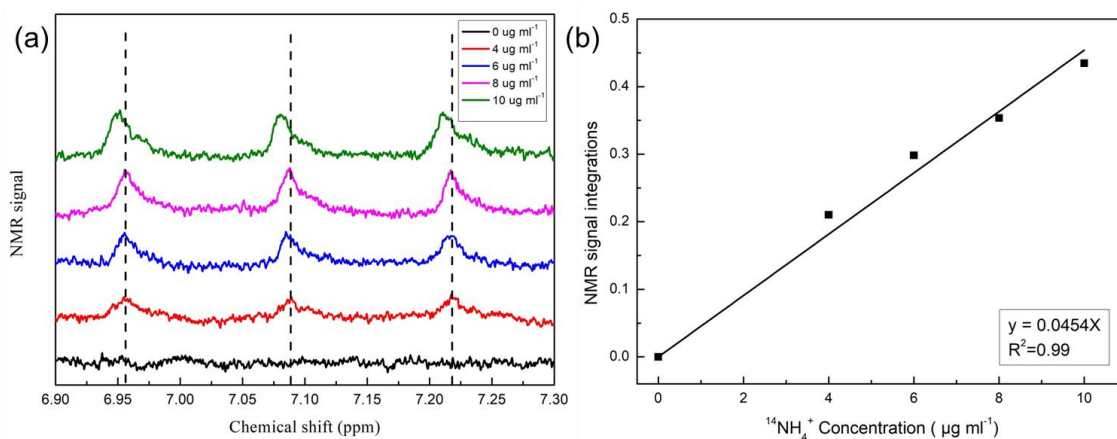Figure S13. (a) NMR spectra of various $(NH_4)_2SO_4$ concentrations. (b) Plots of peak intensity as function of $(NH_4)_2SO_4$ concentrations.
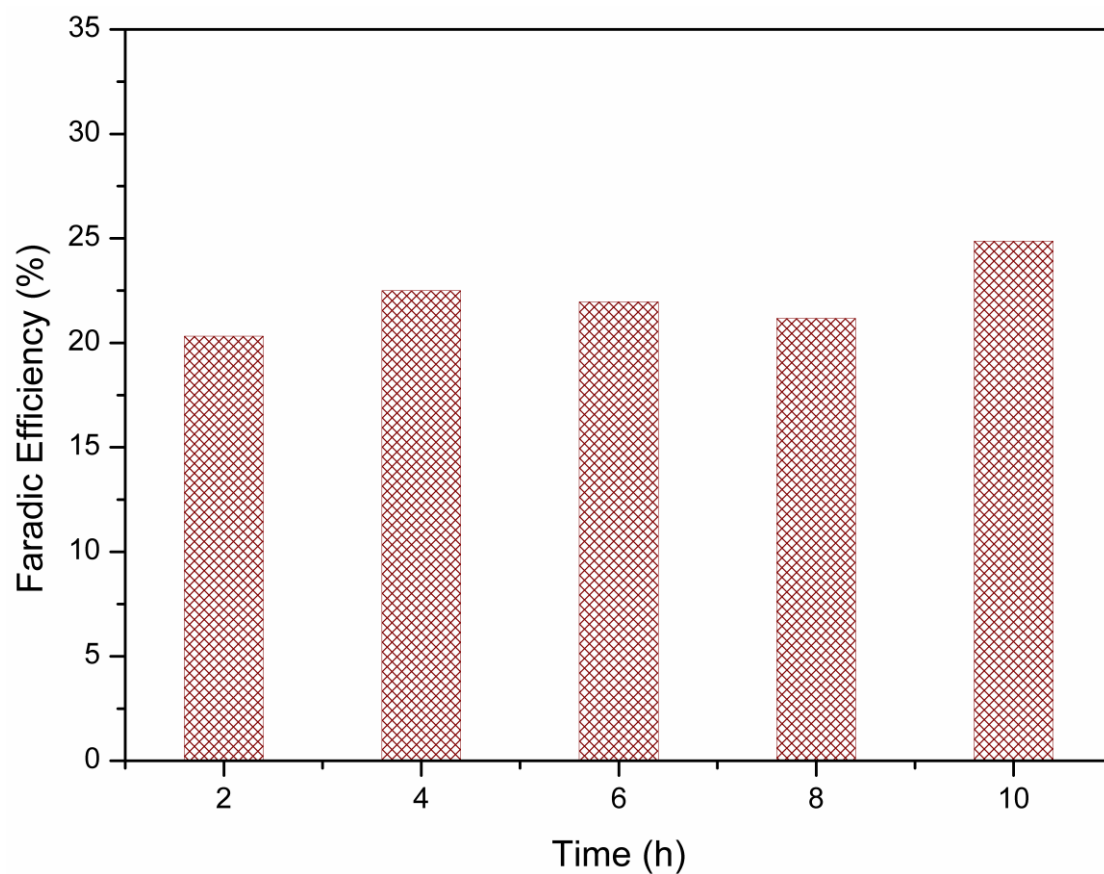
Figure S14. Faradic efficiency of F-MoS$_2$ toward NRR during the 10 h durability test at −0.2 V vs. RHE.

Table S1. Comparison of electrocatalytic N_2 reduction performance of F-MoS2 with recently developed cost-effective electrocatalystsin acidic conditions.

Catalyst	ELectrolyte	FE%	NH_3 ($\mu g\ h^{-1}$ $mg_{cat.}^{-1}$)	Ref.
F-MoS₂	0.05 H_2SO_4	20.6	35.7	This work
NbO_2 nanoparticles	0.05 M H_2SO_4	19.7	11.6	[1]
B_4C nanosheet	0.1 M HCl	15.95	26.57	[2]
N-deficient Mo_2N	0.1 HCl	4.5	78.4	[3]
$Bi_4V_2O_{11}/CeO_2$	0.1 M HCl	10.16	23.21	[4]
S-G	0.1 M HCl	11.5	27.3	[5]
NC	0.1 M HCl	12.3	3.87	[6]
Mo nanofilm	0.01 M H_2SO_4	0.72	1.89 $\mu g\ h^{-1}\ cm^{-2}$	[7]
O-CN	0.1 M HCl	4.97	20.15	[8]
FL-BP	0.01 M HCl	5.07	31.37	[9]
NPC	0.005 M H_2SO_4	9.98	22.2	[10]
PCN	0.1 M HCl	11.59	8.09	[11]
MoN	0.1 M HCl	1.15	18.42 $\mu g\ h^{-1}\ cm^{-2}$	[12]
N, P doped C	0.1 M HCl	4.2	0.97	[13]
N-doped porous carbon	0.05 M H_2SO_4	1.42	23.8	[14]

References

[1]   L. Huang, J. Wu, P. Han, A. M. Al-Enizi, T. M. Almutairi, L. Zhang, G. Zheng, *Small Methods* **2018**, *3*, 1800386.

[2]   W. Qiu, X.-Y. Xie, J. Qiu, W.-H. Fang, R. Liang, X. Ren, X. Ji, G. Cui, A. M. Asiri, G. Cui, B. Tang, X. Sun, *Nat. Commun.* **2018**, *9*, 3485.

[3]   X. Ren, G. Cui, L. Chen, F. Xie, Q. Wei, Z. Tian, X. Sun, *Chem. Commun.* **2018**, *54*, 8474-8477.

[4]   C. Lv, C. Yan, G. Chen, Y. Ding, J. Sun, Y. Zhou, G. Yu, *Angew. Chem. Int. Ed.* **2018**, *57*, 6073-6076.

[5]   L. Xia, J. Yang, H. Wang, R. Zhao, H. Chen, W. Fang, A. M. Asiri, F. Xie, G. Cui, X. Sun, *Chem. Commun.* **2019**, *55*, 3371-3374.

[6]   Q. Qin, T. Heil, M. Antonietti, M. Oschatz, *Small Methods* **2018**, *2*, 1800202.

[7]   D. Yang, T. Chen, Z. Wang, *J. Mater. Chem. A* **2017**, *5*, 18967-18971.

[8]   H. Huang, L. Xia, R. Cao, Z. Niu, H. Chen, Q. Liu, T. Li, X. Shi, A. M. Asiri, X. Sun, *Chem. Eur. J.* **2019**, *25*, 1914-1917.

[9]   L. Zhang, L.-X. Ding, G.-F. Chen, X. Yang, H. Wang, *Angew. Chem.* **2019**, *131*, 2638-2642.

[10]   C. Zhao, S. Zhang, M. Han, X. Zhang, Y. Liu, W. Li, C. Chen, G. Wang, H. Zhang, H. Zhao, *ACS Energy Lett.* **2019**, *4*, 377-383.

[11]   C. Lv, Y. Qian, C. Yan, Y. Ding, Y. Liu, G. Chen, G. Yu, *Angew. Chem. Int. Ed.* **2018**, *57*, 10246-10250.

[12]   L. Zhang, X. Ji, X. Ren, Y. Luo, X. Shi, A. M. Asiri, B. Zheng, X. Sun, *ACS Sustain. Chem. Eng.* **2018**, *6*, 9550-9554.

[13]   P. Song, H. Wang, L. Kang, B. Ran, H. Song, R. Wang, *Chem. Commun.* **2019**, *55*, 687-690.

[14]   Y. Liu, Y. Su, X. Quan, X. Fan, S. Chen, H. Yu, H. Zhao, Y. Zhang, J. Zhao, *ACS Catal.* **2018**, *8*, 1186-1191.